Journal of Sound and Vibration (2002) **254**(5), 877–895
doi:10.1006/jsvi.2001.4133, available online at http://www.idealibrary.com on IDEAL®

ROBUST VIBRATION CONTROL OF A BEAM USING THE H_∞-BASED CONTROLLER WITH MODEL ERROR COMPENSATOR

D.-A. Wang and Y.-M. Huang

Department of Mechanical Engineering, National Central University, Chung-Li, Taiwan, 320 Republic of China. E-mail: t330005@cc.ncu.edu.tw

(*Received* 27 *February* 2001, *and in final form* 4 *September* 2001)

The vibration control of a flexible beam subjected to arbitrary, unmeasurable disturbance forces is investigated in this paper. The beam is analyzed by using modal expansion theorem. The independent modal space control is adopted for the active vibration control. Discrete sensors and actuators are used here. The modal filters are used as the state estimator to obtain the modal co-ordinates and modal velocities for the state feedback control. Because of the existence of the disturbance forces, the vibration control only with the state feedback control law cannot suppress the vibration well. The method of disturbance forces cancellation is then added in the feedback loop. In order to implement the disturbance forces cancellation, the unknown disturbance forces must be observed. The model error compensator is employed to observe the unknown disturbance modal forces for the direct cancellation. After the implementation of the disturbance modal forces cancellation, there are still some residual disturbance modal forces which excite the beam. The disturbance attenuation problem is of concern in the design of the state feedback control law. For ensuring that influence of the residual disturbance modal forces is reduced to an acceptable level, the robust static H_∞ state feedback controller is designed. The vibration control performances of the feedback control with the H_∞ controller and the disturbance forces cancellation are discussed.

1. INTRODUCTION

Vibration control of flexible structures is an important issue in many engineering applications, especially for the precise operation performances in aerospace systems, satellites, flexible manipulators, etc. The flexible structures consist of infinite number of modes and are always having low flexible rigidity and small material damping. A little excitation may lead to large-amplitude vibration and long vibration decay time, and then the challenge is always encountered in the vibration control design. Two types of control methods, i.e., passive control and active control, are generally used. The passive vibration control methods employ the passive elements, e.g., masses, dampers and springs, to adjust the characteristics of controlled structures to the desired values. Different from the passive methods, the active vibration control supplies energy to suppress the vibration. The passive vibration control is simple but sometimes it cannot meet the required control performance. When better control performance is required, the active control is a selection. The implementation of active vibration control needs lots of techniques involving the measurement system, actuator elements and the controller design. During the past several years, active vibration control has become realizable due to the advancements in the relative hardware and software techniques.

There were many researches on the active vibration control in the past years. Balas [1] and Meirovitch *et al.* [2, 3] proposed the concept of the independent modal space control (IMSC) for the flexible structures, where the structures were discretized by the modal expansion method, and the modal feedback control was applied. Every mode is uncoupled in the modal space and is individually controlled. The modal co-ordinates were extracted either by the Kalman filter and Luenberger filter or by the modal filters in their studies. The observation and control spillover concepts were also introduced in their researches. From references [1–3], the modal space vibration control only with the state feedback is useful for the suppression of structures vibration without any disturbance forces. When the structures are excited by external disturbances, vibration control often focuses on isolating the structures from the disturbances, or confining the vibration to certain unimportant areas of the structures [4, 5]. However, it is impossible to completely isolate the structures from the undesired excitation. There is still some excitation transmitted into the structures. When high operation performances of the structures are required, the control algorithm only with the state feedback cannot suppress the external excitation well. In order to reduce the influence of the external excitation, we desire to cancel out the disturbance modal forces by the feedback loop. If the applied disturbance modal forces can be observed, the observed disturbance modal forces can be used in the feedback loop to eliminate the undesired disturbances directly. The vibration of structures then can be greatly suppressed. There have been many works that have observed the unknown disturbances [6, 7]. But the difficulty imposed by these methods is that some level of differentiation of the measured signals is necessary, and the noise will be amplified. Recently, Tu *et al.* [8] developed a model error compensator (MEC), which can observe the unknown disturbances and no differentiation of the measured signals is required. Then it is suitable to employ the MEC as the disturbance force observer in our paper to observe the unknown disturbance modal forces for the direct disturbances cancellation in the feedback control loop.

In this paper an active control procedure to reduce the vibration of a beam subjected to arbitrary, unmeasurable disturbance forces is studied. A Euler beam is considered. The IMSC method is selected as the framework of the control algorithm. The MEC is employed as the disturbance force observer. The feedback control with the combination of the state feedback control law and the MEC is implemented. The modal filters are used as the state estimator of the modal space. Although the disturbance modal forces are directly canceled out by the observed disturbance modal forces, there are still some residual disturbance modal forces which excite the beam. In order to ensure the disturbance attenuation ability of the state feedback controller, the robust H_∞ controller synthesis methodology is applied in this research. The control algorithm is derived from the static H_∞ state feedback control method [9, 10]. The discussions are concentrated on the effect of observing the disturbance modal forces by the MEC and the control performances of the feedback control with MEC.

2. EQUATION OF MOTION

In this paper a slender, cantilever beam with constant cross-section area and length L, shown in Figure 1, is considered. The axial direction is defined as the x-axis and t represents time. Displacement in the transverse direction is denoted as $y(x, t)$. The distributed excitation force acting on the beam is $P(x, t)$. The equation of motion of the beam can be expressed as [11]

$$EI\frac{\partial^4 y}{\partial x^4} + m\frac{\partial^2 y}{\partial t^2} = P(x, t), \tag{1}$$

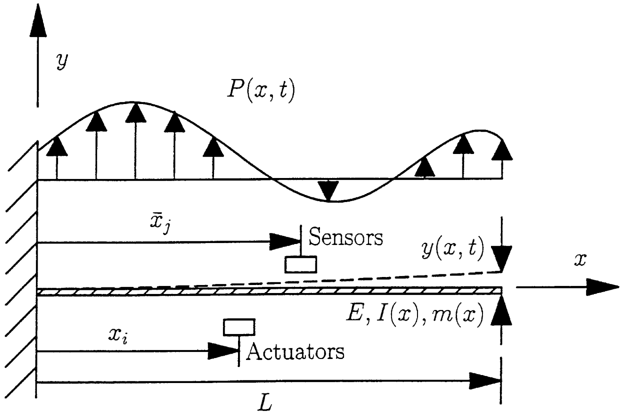

Figure 1. The cantilever beam model with the dislocation sensors and actuators.

where the Euler beam model is used. The notation E is Young's modulus of the beam material, I is the area moment of inertia of the beam cross-section, and m is the mass per unit length. Defining the following dimensionless parameters:

$$y^* = y/L, \quad x^* = x/L, \quad t^* = (\sqrt{EI/m}/L^2)t, \quad P^* = (L^3/EI)P(x,t) \tag{2}$$

we have the non-dimensional equation of motion

$$\frac{\partial^4 y^*}{\partial x^{*4}} + \frac{\partial^2 y^*}{\partial t^{*2}} = P^*. \tag{3}$$

The normalized mode shape corresponding to the rth mode of the dimensionless cantilever beam is written as

$$Y_r^* = A_r^*(\sin \beta_r^* - \sinh \beta_r^*)(\sin \beta_r^* x^* - \sinh \beta_r^* x^*) + (\cos \beta_r^* + \cosh \beta_r^*)(\cos \beta_r^* x^* - \cosh \beta_r^* x^*) \tag{4}$$

with $r = 1, 2, 3, \ldots$ and A_r^* is a constant. In the above expression, the rth eigenvalue of the dimensionless beam β_r^* should satisfy the characteristic equation $\cos \beta_r^* \cosh \beta_r^* = -1$. The natural frequency of the rth mode is $\omega_r^* = \beta_r^{*2}$. For obtaining the time responses of the dimensionless beam subjected to the dimensionless distributed force P^*, the method of truncated modal expansion is adopted here. The dimensionless displacement of the beam is approximately expressed as

$$y^* = \sum_{r=1}^{n} Y_r^* \eta_r^*, \tag{5}$$

where η_r^* is the rth modal co-ordinate, and n is the number of modes used. An extra modal damping term of damping ratio ξ_r^* is added to each modal equation for representing the structure damping. A set of uncoupled modal equations can then be obtained as

$$\ddot{\eta}_r^* + 2\xi_r^* \omega_r^* \dot{\eta}_r^* + \omega_r^{*2} \eta_r^* = n_r^* \tag{6}$$

in which $r = 1, 2, \ldots, n$, and $n_r^* = \int_0^1 Y_r^* P^* \,\mathrm{d}x^*$ is the corresponding modal force. In the following sections all the statements are discussed in this dimensionless system.

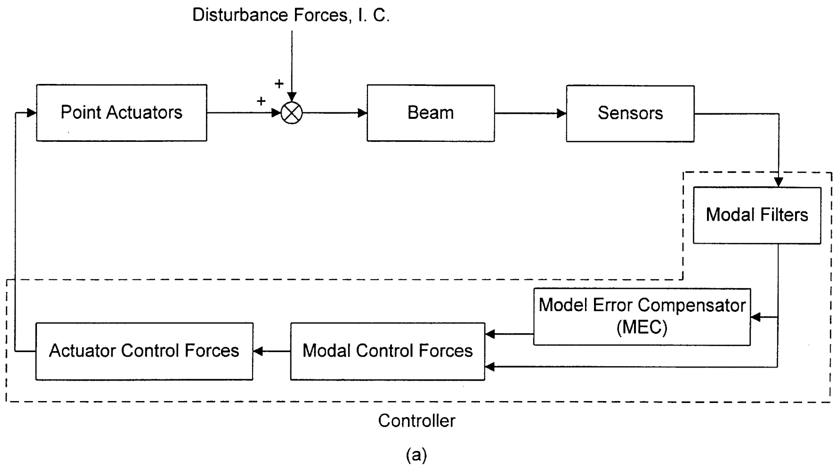

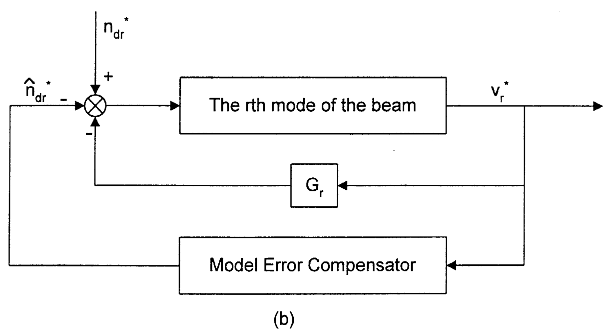

Figure 2. The modal space vibration control block diagram of the beam: (a) schematic diagram of the beam vibration control; (b) the control block diagram of the rth mode of the beam.

3. INDEPENDENT MODAL SPACE CONTROL

The scheme of control applied to the flexible beam here is based on the IMSC method [1–3]. Every mode of the beam is independent, in this method, and is individually controlled. The schematic diagram of the beam vibration control is shown in Figure 2(a). The beam displacements and velocities are measured by discrete sensors. These data are treated through the modal filters. Then the modal co-ordinates and modal velocities can be calculated. The feedback control algorithm is applied in this research. A MEC method [8], discussed later, is presented. This technique is used as the disturbance forces the observer to observe the disturbance modal forces. The observed disturbance modal forces will be included in the feedback loop to suppress the responses of the beam due to the disturbance forces. Then, combining the observed disturbance modal forces and the state feedback control law together, we can obtain the control modal forces. Finally, the control modal forces are transferred to the point actuators for reducing the beam vibration.

3.1. INDEPENDENT MODAL SPACE CONTROL

Since the distributed force P^* applied to the beam is the sum of the unmeasurable disturbance forces and the control forces, the rth modal force n_r^* of the beam can also be separated into two portions. One is the control modal force n^*_{cr} and the other is the disturbance modal force n^*_{dr}. Here, n^*_{dr} is a bounded input, but the bound is unknown.

It is convenient to rearrange each modal equation, given in equation (6), in the state-space form

$$\dot{\mathbf{v}}_r = \mathbf{A}_r\mathbf{v}_r + \mathbf{B}_r n^*_{cr} + \mathbf{C}_r n^*_{dr} \tag{7}$$

in which

$$\mathbf{v}_r = \begin{Bmatrix} \eta^*_r \\ \dot{\eta}^*_r \end{Bmatrix}_{2\times 1}, \quad \mathbf{A}_r = \begin{bmatrix} 0 & 1 \\ -\omega^{*2}_r & -2\xi^*_r\omega^*_r \end{bmatrix}_{2\times 2}, \quad \mathbf{B}_r = \begin{Bmatrix} 0 \\ 1 \end{Bmatrix}_{2\times 1} = \begin{Bmatrix} 0 \\ 1 \end{Bmatrix}_{2\times 1}. \tag{8}$$

In order to reduce the influence of n^*_{dr}, an observed disturbance modal force $\hat{n}^*_{dr}$ is introduced in the feedback loop to cancel the undesired disturbance. This observed disturbance modal force $\hat{n}^*_{dr}$ is included in the control modal force n^*_{cr}.

According to the method of IMSC, each vibration mode is separately controlled. If the state feedback law is chosen, the control modal force could be written as

$$\begin{aligned} n^*_{cr} &= -g_{1r}\eta^*_r - g_{2r}\dot{\eta}^*_r - \hat{n}^*_{dr} \\ &= -\mathbf{G}_r\mathbf{v}_r - \hat{n}^*_{dr}, \end{aligned} \tag{9}$$

in which $\mathbf{G}_r = [g_{1r}\ g_{2r}]_{1\times 2}$ are control gains to be determined. Then, the modal equations with control can still be uncoupledly solved. Figure 2(b) shows the block diagram of the control of the rth mode.

3.2. POINT ACTUATORS FORCES AND MODAL FILTERS

In the practice of vibration control of a distributed structure by the IMSC method, the modal control forces can be approximated by using a finite number of point actuators. Suppose m discrete actuators are used at the points x^*_i, $i = 1, 2, \cdots, m$, to control the first m modes of the beam, the dimensionless control force is expressed as $\mathbf{F}^* = \mathbf{Y}^{*-1}\mathbf{N}^*_c$, where

$$\mathbf{N}^*_c = \begin{bmatrix} n^*_{c1} \\ n^*_{c2} \\ \vdots \\ n^*_{cm} \end{bmatrix}_{m\times 1}, \quad \mathbf{Y}^* = \begin{bmatrix} Y^*_1(x^*_1) & Y^*_1(x^*_2) & \cdots & Y^*_1(x^*_m) \\ Y^*_2(x^*_1) & Y^*_2(x^*_2) & \cdots & Y^*_2(x^*_m) \\ \vdots & \vdots & \vdots & \vdots \\ Y^*_m(x^*_1) & Y^*_m(x^*_2) & \cdots & Y^*_m(x^*_m) \end{bmatrix}_{m\times m}, \quad \mathbf{F}^* = \begin{bmatrix} F^*_1 \\ F^*_2 \\ \vdots \\ F^*_m \end{bmatrix}_{m\times 1}, \tag{10}$$

and F^*_i is the ith dimensionless actuator force. The actuator locations x^*_i must be carefully chosen to avoid the singularity of $\mathbf{Y}^{*-1}$.

The modal co-ordinates are not physical co-ordinates and therefore cannot be measured directly. Theoretically, the modal co-ordinate and the modal velocity associated to the rth mode can be calculated numerically by using the following integration forms:

$$\eta^*_r = \int_0^1 Y^*_r y^*\,\mathrm{d}x^*, \quad \dot{\eta}^*_r = \int_0^1 Y^*_r \dot{y}^*\,\mathrm{d}x^*, \tag{11}$$

where the distributed sensors are needed. Since the distributed sensors are not always available, discrete sensors are usually used. Suppose the displacements of the beam can only be obtained at certain points $\bar{x}^*_j$, $j = 1, 2, \ldots, k$, where k discrete sensors are used, and the first k modal co-ordinates will be estimated. The estimated modal co-ordinates $\hat{\eta}^*_r$ and modal velocities $\dot{\hat{\eta}}_r^*$ based on discrete measurements become [12]

$$\begin{aligned}\hat{\eta}_r^* &= \textstyle\sum_{j=1}^{k}(\mathbf{D}^{*-1})_{rj}\, y^*(\bar{x}_j^*, t^*),\\ \dot{\hat{\eta}}_r^* &= \textstyle\sum_{j=1}^{k}(\mathbf{D}^{*-1})_{rj}\, \dot{y}^*(\bar{x}_j^*, t^*),\end{aligned} \tag{12}$$

where $r = 1, 2, \ldots, k$ and

$$\mathbf{D}^* = \begin{bmatrix} Y_1^*(\bar{x}_1^*) & Y_2^*(\bar{x}_1^*) & \cdots & Y_k^*(\bar{x}_1^*) \\ Y_1^*(\bar{x}_2^*) & Y_2^*(\bar{x}_2^*) & \cdots & Y_k^*(\bar{x}_2^*) \\ \vdots & \cdots & \cdots & \vdots \\ Y_1^*(\bar{x}_k^*) & Y_2^*(\bar{x}_k^*) & \cdots & Y_k^*(\bar{x}_k^*) \end{bmatrix}_{k\times k}. \tag{13}$$

Note that the inverse of $\mathbf{D}^*$ must exist. The estimated modal co-ordinates and modal velocities will replace η_r^* and $\dot{\eta}_r^*$, $r = 1, 2, \ldots, k$, in equation (9) when the control modal force is applied.

The modal equations of the beam, equation (6), are valid for both the controlled and the uncontrolled modes. Then, the associated second order modal equations with control loops can be written as

$$\begin{aligned}\ddot{\mathbf{V}}_c + \mathbf{\Xi}_c\dot{\mathbf{V}}_c + \mathbf{\Omega}_c\mathbf{V}_c &= \mathbf{N}_c + \mathbf{N}_{dc}\\ \ddot{\mathbf{V}}_u + \mathbf{\Xi}_u\dot{\mathbf{V}}_u + \mathbf{\Omega}_u\mathbf{V}_u &= \mathbf{N}_u + \mathbf{N}_{du},\end{aligned} \tag{14}$$

where the subscripts c and u refer to the controlled and uncontrolled modes respectively. Notations $\mathbf{V}$, $\mathbf{\Xi}$, $\mathbf{\Omega}$, $\mathbf{N}$ and $\mathbf{N}_d$ are the modal co-ordinate vector, diagonal modal damping matrix, diagonal modal natural frequency matrix, control modal force vector, and the external disturbance modal force vector respectively. From equation (14), the effects of observation and control spillover can be discussed. The observation spillover and control spillover are inherent characteristics in structural vibration control. The observation spillover occurs when the unobserved modes responses are embedded into the modal filtering. This spillover effect can reduce the accuracy of estimated modal co-ordinates and modal velocities, and can shift the uncontrolled modes eigenvalues when the feedback control is applied [1–3, 12]. The observation spillover may even induce the instability of the system. The selection of sensor positions plays an important role in the phenomenon of observation spillover [3, 12]. Usually, the lower vibration modes dominate the responses of structures. When the sensors are placed at the nodes of the lowest unobserved mode, the amplitude contribution of the unobserved modes to the modal filters can be greatly decreased. Consequently, the observation spillover is reduced. Other useful ways to eliminate the observation spillover involve the use of the prefilters to screen out the contribution of the unobserved modes or the use of more sensors to interpolate the modal co-ordinates precisely [1–3, 12]. The other issue, control spillover, occurs when $\mathbf{N}_u \neq \mathbf{0}$, in equation (14). The actuator forces for the controlled modes can excite the uncontrolled modes. The control spillover phenomenon can be reduced by placing the actuators at the nodes of the lowest uncontrolled mode [3]. The control spillover only degrades the performance of the control responses but cannot destabilize the system [1–3].

4. H_∞ CONTROLLER DESIGN

Every vibration mode is individually controlled in the IMSC. From equations (7)–(9), some undesired excitation from the residual disturbance modal force $n_{dr}^* - \hat{n}_{dr}^*$ still exists

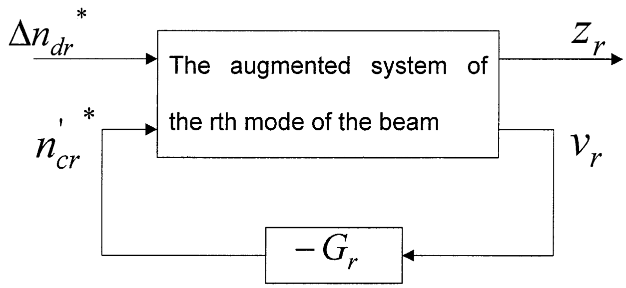

Figure 3. The framework of the static state feedback H_∞ control system.

when the control modal force n_{cr}^* is applied. The selection of the control gains $\mathbf{G}_r$ must ensure a suitable disturbance attenuation ability for the controlled mode. The H_∞ controller design is then adopted here.

In this section, the static state feedback H_∞-based robust controller design is briefly discussed. The H_∞ norm of a stable transfer matrix $\mathbf{T}_r(s)$ is defined as its largest singular value over the entire frequency range, i.e.,

$$\|\mathbf{T}_r(jw)\|_\infty = \sup_\omega \bar{\sigma}[\mathbf{T}_r(jw)], \tag{15}$$

where $\bar{\sigma}$ represents the largest singular value of $\mathbf{T}_r(jw)$. In the H_∞-based control system design, a controller is selected to internally stabilize the system in such a way that the H_∞ norm of a transfer matrix, which describes certain design objectives, is minimized (or becomes smaller than a specified value).

When the observed disturbance modal force $\hat{n}_{dr}^*$, obtained from the MEC, is applied in the feedback loop, the modal equation (7) can be rearranged as the following augmented system:

$$\dot{\mathbf{v}}_r = \mathbf{A}_r\mathbf{v}_r + \mathbf{B}_r n_{cr}^{\prime *} + \mathbf{C}_r \Delta n_{dr}^*,$$

$$\mathbf{z}_r = \mathbf{E}_{1r}\mathbf{v}_r + \mathbf{E}_{2r} n_{cr}^{\prime *}, \tag{16}$$

in which $n_{cr}^{\prime *} = -\mathbf{G}_r\mathbf{v}_r$, $\Delta n_{dr}^* = n_{dr}^* - \hat{n}_{dr}^*$ and $\mathbf{z}_r$ is the defined controlled output. The defined control output $\mathbf{z}_r$ includes two portions, $\mathbf{E}_{1r}\mathbf{v}_r$ and $\mathbf{E}_{2r} n_{cr}^{\prime *}$. In this study the first term indicates the restriction of the magnitudes of state responses where $\mathbf{E}_{1r}$ is the associated weighting matrix. The second term indicates the constraint of the magnitudes of control forces where $\mathbf{E}_{2r}$ is the associated weighting matrix. The static state feedback control is applied. Figure 3 shows the framework of the static state feedback H_∞ control problem. Define the transfer matrix $\mathbf{T}_r(s) \equiv (\mathbf{E}_{1r} - \mathbf{E}_{2r}\mathbf{G}_r)(s\mathbf{I}_n - \mathbf{A}_r + \mathbf{B}_r\mathbf{G}_r)^{-1}\mathbf{C}_r$, which denotes the closed-loop transfer matrix from the residual disturbance modal force Δn_{dr}^* to the controlled output $\mathbf{z}_r$. The problem now is to design a static state feedback control law $n_{cr}^{\prime *} = -\mathbf{G}_r\mathbf{v}_r$ such that the following objectives are achieved:

(1) The closed-loop matrix $\mathbf{A}_r - \mathbf{B}_r\mathbf{G}_r$ is stable.
(2) $\|\mathbf{T}_r(s)\|_\infty < \gamma_r$, where γ_r is a specified value.

The $\|\mathbf{T}_r(s)\|_\infty$ is an appropriate measurement of the influence on the disturbance on the system output. Although the bounded property of $\|\Delta n_{dr}^*\|_2$ is not guaranteed, the controller derived from the transfer matrix $\mathbf{T}_r(s)$ is still applicable. An algebraic Riccati equation approach to find the H_∞ control gains [9] is employed, where the static state feedback control law is obtained by solving a single Riccati equation. If the following Riccati equation

$$\mathbf{A}_r^{\mathrm{T}}\mathbf{X}_r + \mathbf{X}_r\mathbf{A}_r + \gamma_r^{-2}\mathbf{X}_r\mathbf{C}_r\mathbf{C}_r^{\mathrm{T}}\mathbf{X}_r - \frac{1}{\varepsilon_{1r}}\mathbf{X}_r\mathbf{B}_r\mathbf{B}_r^{\mathrm{T}}\mathbf{X}_r + \mathbf{E}_{1r}^{\mathrm{T}}\mathbf{E}_{1r} + \varepsilon_{1r}\mathbf{I}_n = 0 \tag{17}$$

has a positive definite solution $\mathbf{X}_r$ for some γ_r and ε_{1r}, where $\varepsilon_{1r} > 0$, then the static H_∞ state feedback gains are given by

$$\mathbf{G}_r = \frac{1}{2\varepsilon_{1r}}\mathbf{B}_r^{\mathrm{T}}\mathbf{X}_r \tag{18}$$

such that $\mathbf{A}_r - \mathbf{B}_r\mathbf{G}_r$ is stable and $\|\mathbf{T}_r(s)\|_\infty$ is less than γ_r.

To solve the static state feedback H_∞ control problem, one can simply solve Riccati equation (17) with successively smaller values of γ_r. The following conceptual algorithm can be used to find the H_∞ controller systematically:

(1) Given γ_r.
(2) Let $\varepsilon_{1r} = 1$.
(3) Solve equation (17). If $\mathbf{X}_r > 0$, go to 4. Otherwise, if equation (17) does not have a positive definite symmetric solution even for a sufficiently small $\varepsilon_{1r}(\ll 1)$, then increase γ_r, and go to 2.
(4) If $\gamma_r <$ specified performance level, compute $\mathbf{G}_r$ as in equation (18). Otherwise, decrease γ_r, and go to 2.

The above iterative procedure can also be used to find the infimal of $\|\mathbf{T}_r(s)\|_\infty$ and the associated controller for the optimal disturbance attenuation.

5. MODEL ERROR COMPENSATOR (MEC)

The MEC [8] employed here is a disturbance force observer which can accurately estimate the disturbance modal forces in some prescribed performance bound of disturbance estimation error. The major advantage of the MEC is that no differentiation of the measured signals is required. The idea of MEC is motivated by the invertibility criterion of a linear time-invariant state equation [13]. As pointed out by Moylan [13], if the system is invertible, then it turns out to be possible to reproduce the input functionally from the knowledge of the output. From equation (7), it is evident that n_{dr}^* has the potential to be functionally reproduced if the inverse of equation (7) exists.

Consider the rth modal equation

$$\begin{aligned}\dot{\mathbf{v}}_r &= \tilde{\mathbf{A}}_r\mathbf{v}_r + \mathbf{C}_r n_{dr}^*,\\ \mathbf{z}_{mr} &= \tilde{\mathbf{C}}_{mr}\mathbf{v}_r,\end{aligned} \tag{19}$$

where no observed disturbance modal force is applied. The matrix $\tilde{\mathbf{A}}_r$ is $\tilde{\mathbf{A}}_r = \mathbf{A}_r - \mathbf{B}_r\mathbf{G}_r$, $\mathbf{z}_{mr}$ is the defined measured output for constructing MEC and $\tilde{\mathbf{C}}_{mr}$ is a defined matrix. The vector $\mathbf{z}_{mr}$ and matrix $\tilde{\mathbf{C}}_{mr}$ have appropriate dimensions. Suppose the system, equation (19), is both controllable and observable, and the invertibility of the triple $(\tilde{\mathbf{A}}_r, \mathbf{C}_r, \tilde{\mathbf{C}}_{mr})$ is held. Then, the model error, the disturbance modal force n_{dr}^*, could be approximated by the measured output $\mathbf{z}_{mr}$ [8]. An auxiliary system

$$\begin{aligned}\dot{\hat{\mathbf{v}}}_r &= \tilde{\mathbf{A}}_r\hat{\mathbf{v}}_r,\\ \hat{\mathbf{z}}_{mr} &= \tilde{\mathbf{C}}_{mr}\hat{\mathbf{v}}_r\end{aligned} \tag{20}$$

is established, where n_{dr}^* is not considered. By comparing equation (20) with the system (19), it is clear that in general $\hat{\mathbf{z}}_{mr} \neq \mathbf{z}_{mr}$ because of the existence of n_{dr}^*. According to the invertibility criterion given by Moylan [13], n^*_{dr} is a linear function of $\mathbf{z}_{mr}$. Instead of finding n^*_{dr} directly from $\mathbf{z}_{mr}$, it is suitable to obtain n^*_{dr} from the difference between $\mathbf{z}_{mr}$ and $\hat{\mathbf{z}}_{mr}$ to avoid the differentiation of the measured output signal $\mathbf{z}_{mr}$. A candidate approximation of the model error n^*_{dr} is given by [8]

$$n^*_{dr} \approx \hat{n}^*_{dr} = \tilde{\mathbf{g}}_r(\mathbf{z}_{mr}\text{-}\hat{\mathbf{z}}_{mr}), \tag{21}$$

where $\mathbf{g}_r$ is a matrix. By adding this approximation function to equation (20), the auxiliary system becomes

$$\begin{aligned} \dot{\hat{\mathbf{v}}}_r &= \tilde{\mathbf{A}}_r \hat{\mathbf{v}}_r + \mathbf{C}_r \tilde{\mathbf{g}}_r (\mathbf{z}_{mr} - \hat{\mathbf{z}}_{mr}), \\ \hat{\mathbf{z}}_{mr} &= \tilde{\mathbf{C}}_{mr} \hat{\mathbf{v}}_r. \end{aligned} \tag{22}$$

The above equation is a new model, in which the model error n^*_{dr} has been compensated by $\hat{n}^*_{dr}$. Subtracting equation (22) from equation (19), we have

$$\begin{aligned} \dot{\mathbf{e}}_r &= \tilde{\mathbf{A}}_r \mathbf{e}_r + \mathbf{C}_r \mathbf{e}_{dr}, \\ \mathbf{e}_{zr} &= \tilde{\mathbf{C}}_{mr} \mathbf{e}_r \end{aligned} \tag{23}$$

or

$$\begin{aligned} \dot{\mathbf{e}}_r &= (\tilde{\mathbf{A}}_r - \mathbf{C}_r \tilde{\mathbf{g}}_r \tilde{\mathbf{C}}_{mr}) \mathbf{e}_r + \mathbf{C}_r n^*_{dr}, \\ \mathbf{e}_{zr} &= \tilde{\mathbf{C}}_{mr} \mathbf{e}_r, \end{aligned} \tag{24}$$

where $\mathbf{e}_r = \mathbf{v}_r - \hat{\mathbf{v}}_r$ denotes the state estimation error, $\mathbf{e}_{zr} = \mathbf{z}_{mr} - \hat{\mathbf{z}}_{mr}$ denotes the output estimation error and $\mathbf{e}_{dr} = n^*_{dr} - \tilde{\mathbf{g}}_r \mathbf{e}_{zr}$ is the disturbance estimation error. Equations (23) and (24) are the same but in different forms. Define the following two transfer matrices

$$\mathscr{L}\{\mathbf{e}_{zr}\} = \tilde{\mathbf{T}}_{1r}(s)\ \mathscr{L}\{\mathbf{e}_{dr}\}, \tag{25}$$

where $\tilde{\mathbf{T}}_{1r}(s) = \tilde{\mathbf{C}}_{mr}(s\mathbf{I}_n - \tilde{\mathbf{A}}_r)^{-1}\mathbf{C}_r$; and

$$\mathscr{L}\{\mathbf{e}_{zr}\} = \tilde{\mathbf{T}}_{2r}(s)\,\mathscr{L}\{n^*_{dr}\}, \tag{26}$$

where $\tilde{\mathbf{T}}_{2r}(s) = \tilde{\mathbf{C}}_{mr}[s\mathbf{I}_n - (\tilde{\mathbf{A}}_r - \mathbf{C}_r \mathbf{g}_r \tilde{\mathbf{C}}_{mr})]^{-1}\mathbf{C}_r$. Combining equations (25) and (26), we have

$$\tilde{\mathbf{T}}_{1r}(s)\mathscr{L}\{\mathbf{e}_{dr}\} = \tilde{\mathbf{T}}_{2r}(\mathrm{s})\mathscr{L}\{n^*_{dr}\}. \tag{27}$$

From the above equation, we can design an appropriate $\tilde{\mathbf{g}}_r$ in $\tilde{\mathbf{T}}_{2r}(s)$ to ensure that the disturbance estimation error $\mathbf{e}_{dr}$ is sufficiently small. Hence, the objective of MEC is to find a suitable $\tilde{\mathbf{g}}_r$ in $\tilde{\mathbf{T}}_{2r}(s)$, such that the disturbance estimation error is bounded as

$$\|\mathbf{e}_{dr}(s)\|_2 < \varepsilon_{2r}, \tag{28}$$

where ε_{2r} is a prescribed specification. Moreover, $\|\tilde{\mathbf{T}}_{2r}(s)\|_\infty$ must be bounded as

$$\|\tilde{\mathbf{T}}_{2r}(s)\|_\infty = \|\tilde{\mathbf{C}}_{mr}[s\mathbf{I}_n - (\tilde{\mathbf{A}}_r - \mathbf{C}_r \tilde{\mathbf{g}}_r \tilde{\mathbf{C}}_{mr})]^{-1}\mathbf{C}_r\|_\infty < \frac{\varepsilon_{2r}}{\alpha_r \beta_r}. \tag{29}$$

The factor α_r is associated with the bound of the changing rate of the disturbance modal force, and the factor β_r is associated with the relative H_∞ norm of $\tilde{\mathbf{T}}_{1r}(s)$. The determination of α_r and β_r can be found in reference [8]. Equation (29) becomes the design objective of finding $\tilde{\mathbf{g}}_r$. Matrix $\tilde{\mathbf{g}}_r$ can be determined by the general H_∞ output feedback controller synthesis [14] or a simple method described in reference [8] where the Nelder–Mead simplex algorithm is employed [15]. If no such matrix $\tilde{\mathbf{g}}_r$ can be found, we could relax ε_{2r}, or

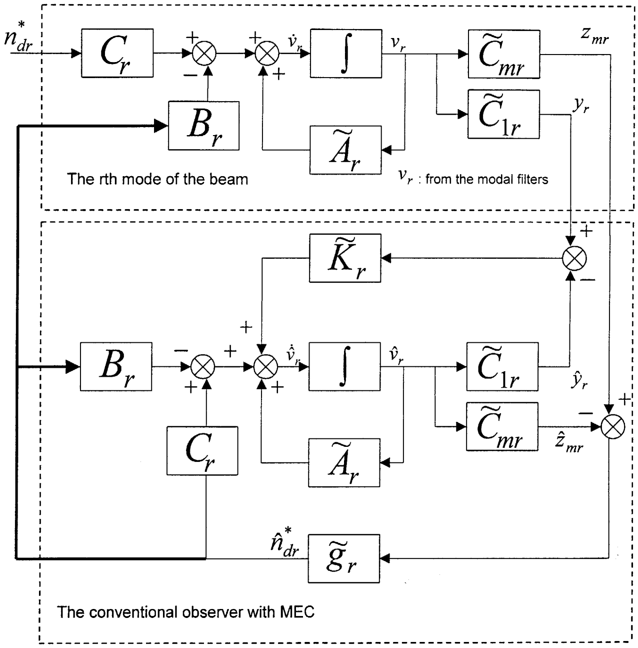

Figure 4. The block diagram of the conventional observer with the model error compensator (MEC).

only minimize $\|\tilde{\mathbf{T}}_{2r}(s)\|_\infty$. The unknown disturbance n^*_{dr} can then be accurately observed by equation (21) when the matrix $\tilde{\mathbf{g}}_r$ is determined. Note that no differentiation is necessary in the calculation of $\hat{n}^*_{dr}$. With the H_∞ control gains determined by equation (18) and the observed disturbance modal force from equation (21), the control modal force, equation (9), can be obtained. The time responses of the beam can also be obtained from equation (5) after controlled modal equations (7) are solved.

The MEC is usually incorporated with the conventional state estimator. Figure 4 illustrates the conjunction block diagram of the estimator system, where the observed disturbance modal force $\hat{n}^*_{dr}$ is used to cancel out n^*_{dr} in the feedback loop. The state $\mathbf{v}_r$ is obtained from the modal filters. The conventional estimator with MEC is described as

$$\begin{aligned}
\dot{\hat{\mathbf{v}}}_r &= \tilde{\mathbf{A}}_r\hat{\mathbf{v}}_r + \tilde{\mathbf{K}}_r(\mathbf{y}_r - \hat{\mathbf{y}}_r) + \mathbf{C}_r\tilde{\mathbf{g}}_r(\mathbf{z}_{mr} - \hat{\mathbf{z}}_{\mathrm{m}r}) \\
&= (\tilde{\mathbf{A}}_r - \tilde{\mathbf{K}}_r\tilde{\mathbf{C}}_{1r})\hat{\mathbf{v}}_r + \mathbf{C}_r\tilde{\mathbf{g}}_r(\mathbf{z}_{mr} - \hat{\mathbf{z}}_{mr}) + \tilde{\mathbf{K}}_r\mathbf{y}_r, \\
\hat{\mathbf{z}}_{mr} &= \tilde{\mathbf{C}}_{mr}\hat{\mathbf{v}}_r, \\
\hat{\mathbf{y}}_r &= \tilde{\mathbf{C}}_{1r}\hat{\mathbf{v}}_r, \\
\hat{\mathbf{n}}^*_{dr} &= \tilde{\mathbf{g}}_r(\mathbf{z}_{mr} - \hat{\mathbf{z}}_{mr}),
\end{aligned} \tag{30}$$

where $\mathbf{y}_r$ is the defined measured output of the system, $\hat{\mathbf{y}}_r$ is the defined measured output of the conventional observer, $\tilde{\mathbf{C}}_{1r}$ is a defined matrix and $\tilde{\mathbf{K}}_r$ is a conventional observer gain. Note that the transfer matrices $\tilde{\mathbf{T}}_{1r}(s)$ and $\tilde{\mathbf{T}}_{2r}(s)$ now should be determined by replacing matrix $\tilde{\mathbf{A}}_r$ with $\tilde{\mathbf{A}}_r - \tilde{\mathbf{K}}_r\tilde{\mathbf{C}}_{1r}$. The error dynamics of this observer system can be found in reference [8]. A two-step observer design strategy [8] is employed here. First, select a suitable $\tilde{\mathbf{C}}_{mr}$ in equation (19) to guarantee the invertibility of the system for constructing the MEC. Second, design a conventional observer and add MEC to the observer, and then determine the MEC gains $\tilde{\mathbf{g}}_r$.

6. NUMERICAL SIMULATION AND DISCUSSIONS

The simulation of the vibration control is carried out in the dimensionless system. A cantilever beam subjected to unmeasurable disturbance forces is considered here. To provide a suitable disturbance attenuation, the static state feedback H_∞ controller is used. The truncated beam model is adopted. The first 10 modes of the beam, including both the controlled and uncontrolled modes, are used to represent the total beam responses in the numerical calculation. The damping ratio ξ_r^* of the modes is $\xi_r^* = 0{\cdot}05$. According to IMSC for distributed structures, each mode is individually controlled. The modal filters are used as the state estimator. The disturbance force observer, MEC, merged in the feedback loop, provides the observed disturbance modal forces for compensating the undesired disturbance modal forces. The initial conditions of the beam are $y^*(1,0) = 0$, $\dot{y}^*(1,0) = 0$ and the disturbance force is applied at the tip of the beam. The ideal sensors and actuators used for the active vibration control are dislocated from each other. The locations of sensors and actuators play a major role in the vibration control effect of structures. Because of the need for observing the disturbance modal forces accurately in this research, the number of observed modes is more than the number of controlled modes. The first four modes are controlled here. The first six modal co-ordinates and modal velocities are observed. The six sensors are distributed near the nodes of the seventh mode, then the observation spillover is largely eliminated. The sensor locations $\bar{x}_j^*$ are (0·19, 0·35, 0·50, 0·65, 0·81, 0·95). For using less actuator forces to control the structure vibration, good locations of the actuators are the points near the antinodes of the controlled mode shapes. The four actuator locations x_i^* are at (0·29, 0·47, 0·69, 1·00), which are the points at which the antinodes of the first three mode shapes occur.

6.1. ESTIMATED STATES BY USING MODAL FILTERS

The purpose of the modal filters is to obtain the modal co-ordinates and modal velocities. Figure 5 illustrates the estimated modal co-ordinates from the modal filters, where the dimensionless disturbance force is $P^* = \sin t^*$ and no control is applied. The estimated modal co-ordinates are shown by the solid lines and the theoretical results are indicated by the dashed lines. From Figure 5(a), it can be seen that the first estimated modal co-ordinate is almost the same as the theoretical value. Figure 5(b) illustrates the fourth estimated modal co-ordinate, in which small observation spillover is found. Figure 5(c) shows the latest estimated modal co-ordinate, the sixth mode. Obviously, the observation spillover is large for this mode. In conclusion, the estimated modal co-ordinates of the lower modes are more accurate than the higher ones [12]. The observation spillover is more evident in higher modes.

6.2. MODAL SPACE VIBRATION CONTROL WITH H_∞ CONTROLLER AND MEC

The estimated modal co-ordinates and velocities in section 3.2 are not only used to generate the control modal forces in the modal space vibration control, but also used as the measured output of the modal equations for constructing the MEC and the conventional observer. The modal control forces consist of the static H_∞ state feedback control law and the observed disturbance modal forces $\hat{n}_{dr}^*$ from MEC. After the modal control forces are obtained, they are transformed by the $\mathbf{Y}^{*-1}$ in equation (10) to generate the point actuators forces which will be applying at the beam.

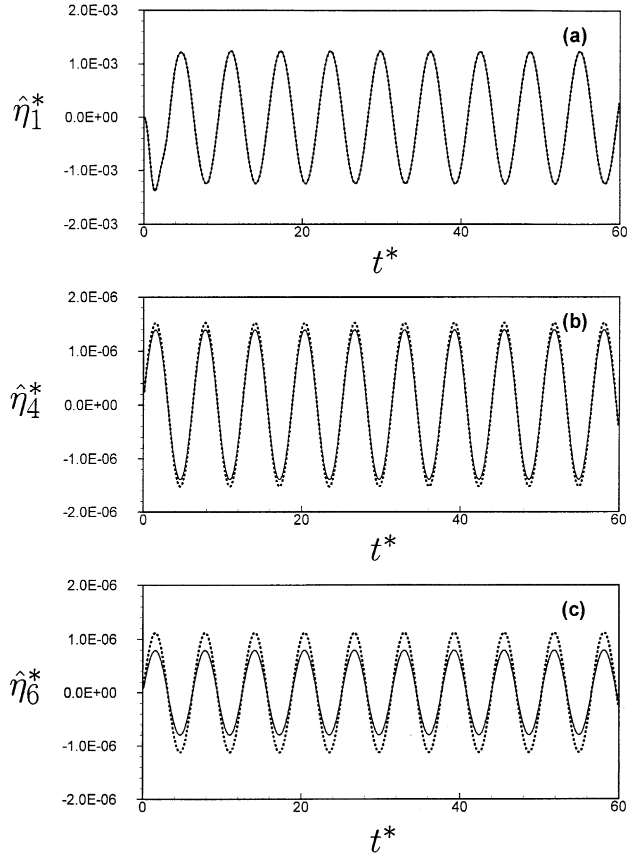

Figure 5. The estimated modal co-ordinates by using modal filters: (a) the first mode; (b) the fourth mode; (c) the sixth mode.

6.2.1. H_∞ *controller design*

The design objective of the H_∞ controller is to find the control gains $\mathbf{G}_r$ which ensure that the closed-loop equations of controlled modes are stable and that $\|\mathbf{T}_r(s)\|_\infty$ are less than γ_r. We select $\mathbf{E}_{1r} = \left[\begin{smallmatrix}1 & 0\\ 0 & 1\end{smallmatrix}\right]$ and $\mathbf{E}_{2r} = [1\ 1]^{\mathrm{T}}$ for all controlled modes. All the magnitudes of modal co-ordinates and velocities have the same weighting. Instead of choosing a prescribed γ_r for the H_∞ controller design, we intend to find the infimal γ_r^* of each controlled mode as the controller design specification. Applying the procedure given in section 4, γ_r^* of the controlled modes and the associated positive definite solutions $\mathbf{X}_r$ of the Riccati equations can be obtained. With the positive definite solutions $\mathbf{X}_r$, the static H_∞ state feedback gains $\mathbf{G}_r$ can be found from equation (18). Then, the modal state space feedback control forces are $n_{cr}'^* = -\mathbf{G}_r\mathbf{v}_r$. Table 1 gives the list of infimal γ_r^* within a tolerance of 0·001 and $\mathbf{G}_r$ for the controlled modes. Figure 6 gives the maximum singular value plots of $\mathbf{T}_r(s)$ of all modes from the modal space viewpoint. The solid line indicates the maximum singular value of the controlled system and the dashed line exhibits the maximum singular value of the uncontrolled system. The H_∞ norm of the lower modes is greater than that of the higher modes. Figure 6 shows that the $\|\mathbf{T}_r(s)\|_\infty$ of the controlled modes are reduced to the associated infimal γ_r^*.

TABLE 1

The infimal γ_r^* of $\|\mathbf{T}_r(s)\|_\infty$ and the associated H_∞ control gains

Mode no.	γ_r^*	$\mathbf{G}_r = [g_{1r} \quad g_{2r}]$
1	0·865	[0·5097 0·8581]
2	0·421	[0·2752 0·6557]
3	0·195	[0·7678 0·5695]
4	0·110	[0·5000 0·5317]

The conventional observer gains $\tilde{\mathbf{K}}_r$ and the MEC gains $\tilde{\mathbf{g}}_r$

Mode no.	$\tilde{\mathbf{K}}_r = [k_{1r} \quad k_{2r}]^T$	$\tilde{\mathbf{g}}_r$
1	$[16{\cdot}97 \quad 86{\cdot}59]^T$	39·5726
2	$[16{\cdot}24 \quad -397{\cdot}30]^T$	39·1891
3	$[14{\cdot}30 \quad -3743{\cdot}71]^T$	38·0664
4	$[11{\cdot}00 \quad -14580{\cdot}00]^T$	35·7151

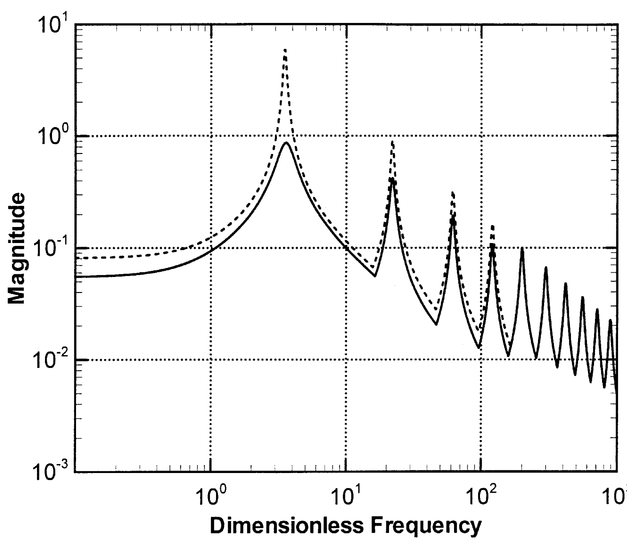

Figure 6. The maximum singular value plot of $\mathbf{T}_r(s)$ of the beam.

6.2.2. *The Model Error Compensator design*

The purpose of the MEC presented in this paper is to observe the unknown disturbance modal forces, which will be used in the feedback loop to cancel out the undesired disturbances. After the design of H_∞ controller, the MEC can be constructed. The MEC proposed here is usually incorporated with the conventional observer. Let $\tilde{\mathbf{C}}_{mr} = [0\ 1]$ for all controlled modes in our case. From the invertibility criterion given by Moylan [13], the modal equation in equation (19) is invertible. The proposed MEC method can then be employed to observe the disturbance modal forces.

Before designing the MEC gains $\mathbf{g}_r$, the conventional observer is designed first. Define $\tilde{\mathbf{C}}_{1r} = [1\ 0]$ for all controlled modes. The modal co-ordinates become the measured output

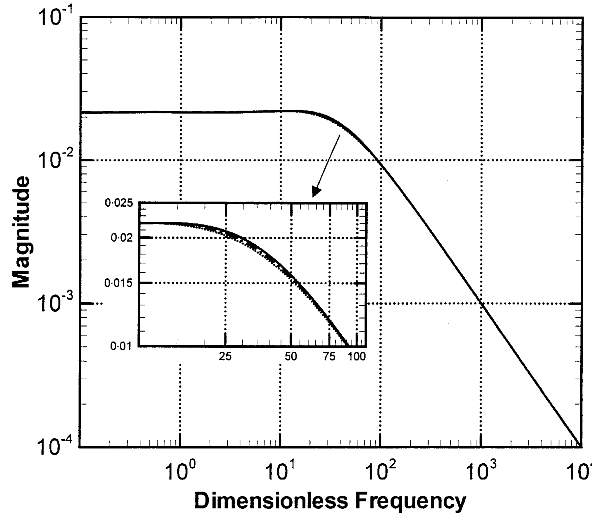

Figure 7. The bode plots of $\tilde{\mathbf{T}}_{2r}(s)$ of the controlled modes.

for constructing the observer. The associated conventional observer gain vectors are $\tilde{\mathbf{K}}_r = [k_{1r}\ k_{2r}]^{\mathrm{T}}$ for the controlled modes. From Figure 4 and the error dynamics analysis given in reference [8], if the gain vectors $\tilde{\mathbf{K}}_r$ are properly designed, then the estimated states $\hat{\mathbf{v}}_r$ will have the tendency to be driven to the actual states $\mathbf{v}_r$. The observed disturbance modal forces are more accurate with the existence of the observer gain vectors $\tilde{\mathbf{K}}_r$. Let the observer poles for all controlled modes have the same values $s_{1,2} = -9 \pm \mathrm{j}6$. The associated observer gain vectors $\tilde{\mathbf{K}}_r$ can be determined and are given in Table 1. With the matrices $\tilde{\mathbf{C}}_{mr}$ chosen before, the associated MEC gains $\tilde{\mathbf{g}}_r$ now are scalars and $\tilde{\mathbf{T}}_{2r}(s)$ are transfer functions. The observed disturbance modal forces are given by $\hat{n}^*_{dr} = \tilde{\mathbf{g}}_r(\mathbf{z}_{mr} - \hat{\mathbf{z}}_{mr}) = \tilde{\mathbf{g}}_r[0\ 1]\,(\mathbf{v}_r - \hat{\mathbf{v}}_r)$. The designed specifications of the disturbance estimation errors are $\|\mathbf{e}_{dr}(s)\|_2 < 0{\cdot}2$ for all controlled modes. Let $\alpha_r = 36{\cdot}37$ and $\beta_r = 0{\cdot}25$ for all controlled modes. Then the corresponding bounds of $\|\tilde{\mathbf{T}}_{2r}(s)\|_\infty$ are less than 0·022. In this paper we adopt a simplex method presented in reference [8] to solve $\tilde{\mathbf{g}}_r$. This method employs the Nelder–Mead simplex algorithm [15], a direct search method, for minimizing a function of several variables. The solutions of $\tilde{\mathbf{g}}_r$ for the controlled modes are given in Table 1. The observed disturbance modal forces $\hat{n}^*_{dr}$ then can be applied in the feedback loop to cancel out the disturbance modal forces n^*_{dr}.

Figure 7 exhibits the bode plots of $\tilde{\mathbf{T}}_{2r}(s)$ for the controlled modes. The solid line, dashed line, dash–dot–dash line and dotted line show the bode plots of $\tilde{\mathbf{T}}_{2r}(s)$ for the first, second, third and fourth modes, respectively. It is seen that $\|\tilde{\mathbf{T}}_{2r}(s)\|_\infty$ are less than the desired upper bound 0·022 when the designed MEC gains $\tilde{\mathbf{g}}_r$ are given, and the prescribed bounded disturbance estimation errors $\|\mathbf{e}_{dr}(s)\|_2 < 0{\cdot}2$ are achieved for all controlled modes. Figure 8 illustrates the performance of the disturbance force observer MEC for observing different types of disturbance forces for the first mode. The effect of tracking the sine function, $\sin t^*$, is shown in Figure 8(a). The solid line displays the observed disturbance modal force $\hat{n}^*_{d1}$. The dashed line indicates the real disturbance modal force n^*_{d1}. Figure 8(b) represents the result of observing the $\sin t^* \cdot \mathrm{e}^{-0{\cdot}5t^*}$, Figure 8(c) shows the result of observing the force $0{\cdot}4 \sin t^* + 0{\cdot}3 \cos 2t^* + 0{\cdot}3 \sin(4t^* + 1)$, and Figure 8(d) illustrates the result of observing the step function of amplitude 1. Good accuracy of observing the disturbance modal forces n^*_{dr} can be achieved by means of the MEC presented. The more accurately the

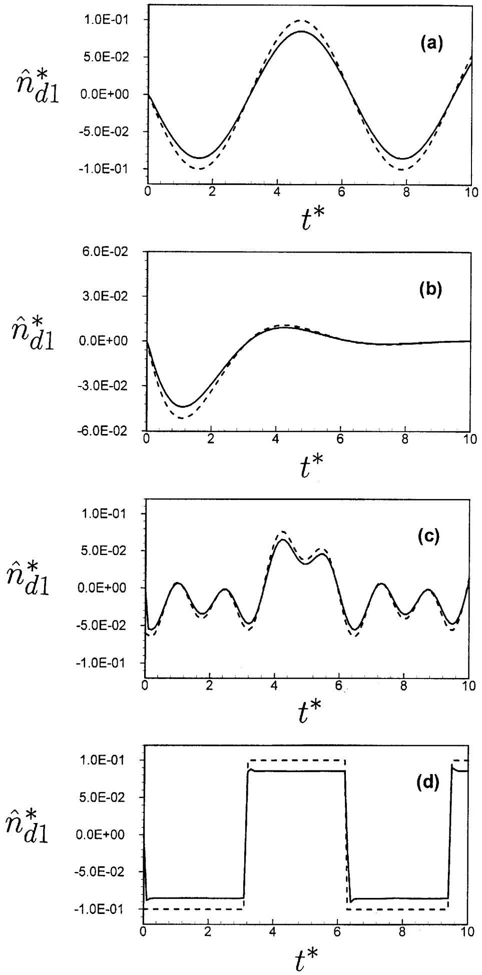

Figure 8. The observed disturbance modal forces via the model error compensator: (a) $\sin t^*$; (b) $\sin t^* \, e^{-0\cdot 5t^*}$; (c) $0\cdot 4 \sin t^* + 0\cdot 3 \cos 2t^* + 0\cdot 3 \sin(4t^* + 1)$; (d) step function of amplitude 1.

disturbance modal forces are observed, the better cancellation of these disturbance forces will be obtained when the feedback control is implemented. From Figure 8, we also see that when the changing rates of the disturbance forces are great, the estimation errors are larger than those when the changing rates are small. The changing rates of the disturbance forces are not predictable, and sometimes they do not satisfy the bounds of the changing rate factor α_r. The MEC method is accurate for observing the disturbance modal forces when the changing rates of the disturbance forces are small. Although some unexpected disturbances perhaps destabilize the control system, the MEC approach can work well in the general engineering applications.

The control modal forces applied in the feedback loop involve the static H_∞ state feedback control law and the observed disturbance modal forces. The static H_∞ state feedback control law provides the optimal disturbance attenuation ability, and the observed disturbance modal forces are used to directly cancel out the undesired disturbances. Figure 9 exhibits the controlled and uncontrolled frequency response function plots of the beam from the tip disturbance force to the tip displacement. The solid line indicates the

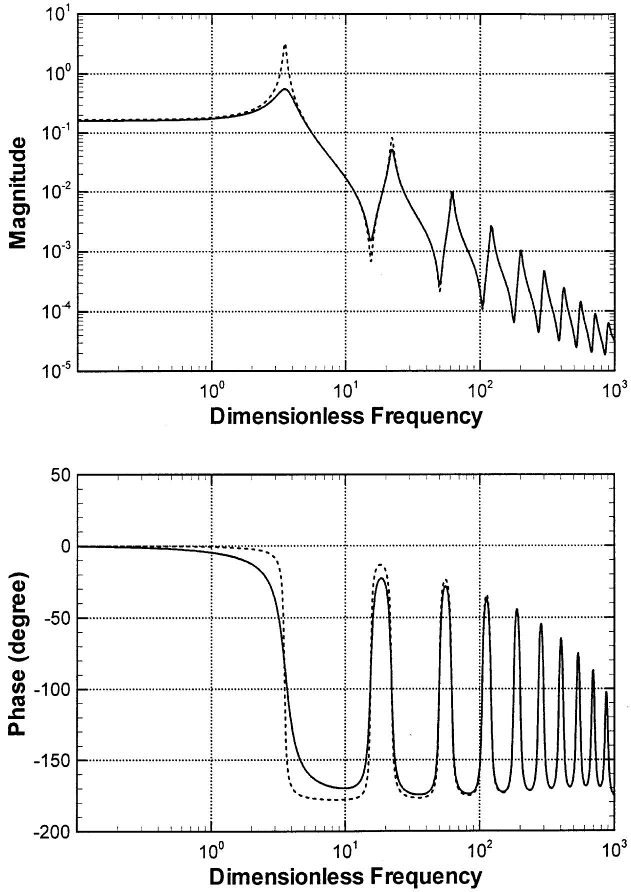

Figure 9. The frequency response function plots of the beam from the tip excitation to the tip displacement.

beam frequency response function plot under the static H_∞ state feedback control. The dashed line displays the uncontrolled beam frequency response function plot. The maximum frequency response of the beam is reduced about 82·9%.

The time-domain control responses are given below. The first four modes of the beam are controlled and the dimensionless disturbance force is $\sin t^*$ if not specified. Figure 10 illustrates the first mode responses of the beam under the modal space vibration control presented in this paper. The controlled responses are shown by the solid lines, and the non-controlled responses are indicated by the dashed lines. It is seen that the static H_∞ state feedback control with MEC can successfully suppress the modal responses. It is also interesting to note that the steady state responses of the first mode are not zero. This is because the disturbance modal force n^*_{d1} has not been entirely eliminated by $\hat{n}^*_{d1}$. The residual disturbance modal force $n^*_{d1} - \hat{n}^*_{d1}$ governs the steady state responses of the first modal equation. Figure 11 shows the beam responses, represented by the solid lines, under the modal space vibration control with the static H_∞ state feedback control law and the MEC. For comparison, the responses of the beam only with the static H_∞ state feedback control are illustrated by the dashed lines, and the non-controlled beam responses are exhibited by the dash–dot–dash lines. From this figure, it is obvious that the vibration control effect of the beam with the disturbance excitation is not good if only the static

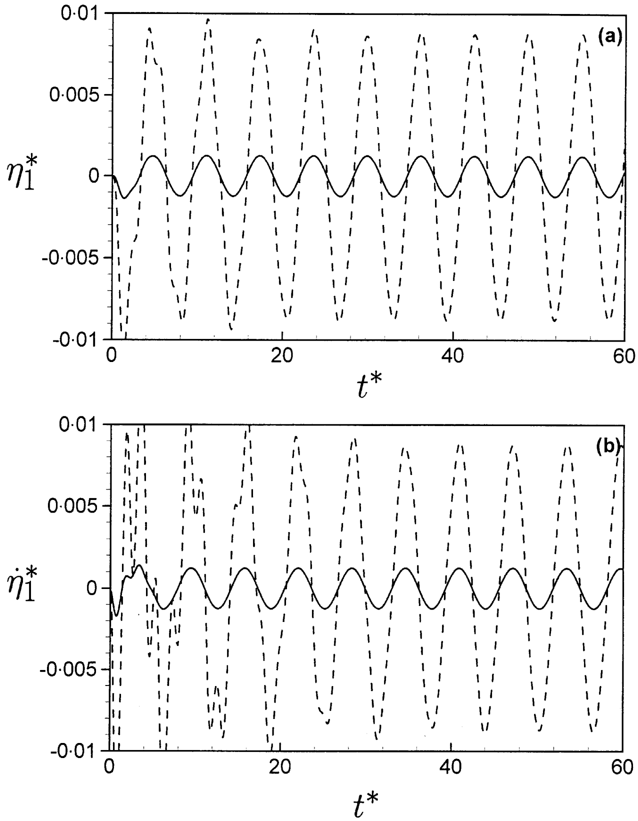

Figure 10. The responses of the first mode under the static H_∞ state feedback control with MEC: (a) modal co-ordinate; (b) modal velocity.

H_∞ state feedback control law is applied. The vibration of the beam excited by the disturbance force can be suppressed well by using the static H_∞ state feedback control law with MEC. There is still some steady state vibration in Figure 11. It includes vibration of the controlled modes, which cannot be entirely suppressed by $\hat{n}_{dr}^*$, and the vibration of uncontrolled modes. The uncontrolled modes are excited by the disturbance forces and the control forces. The responses of the uncontrolled modes induced by the control forces are called the control spillover. The phenomenon of the control spillover is not evident in this case.

7. CONCLUSIONS

Active vibration control of a flexible beam, subjected to unknown disturbance forces, has been investigated. The independent modal space control is used as the frame of the vibration control of the distributed parameters structure. Discrete sensors and actuators are used. The modal filters are used for estimating the modal coordinates. The number of sensors are more than the number of controlled modes for reducing the observation spillover. The robust H_∞-based controller with the model error compensator is applied to suppress the beam vibration. The model error compensator is used as the disturbance force observer to observe the unknown disturbance modal forces in some prescribed performance

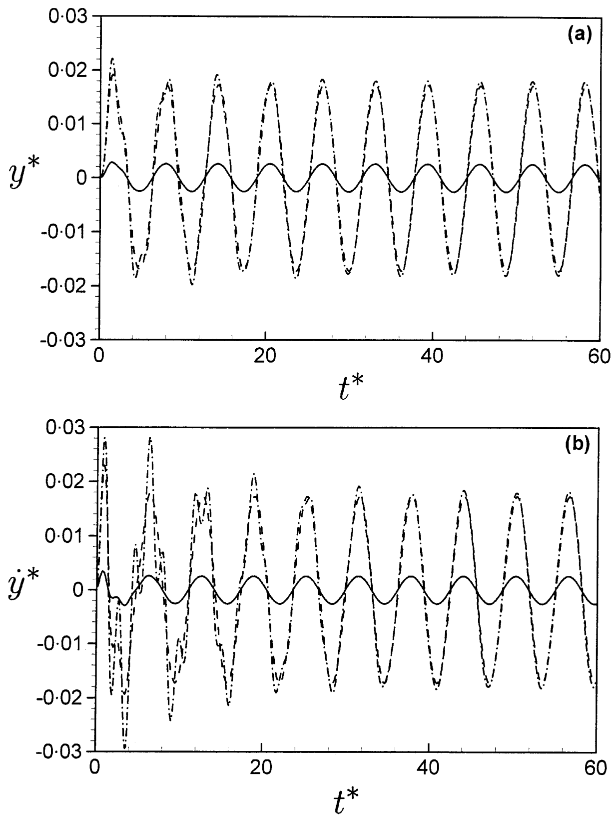

Figure 11. The tip responses of the beam under the static H_∞ state feedback control with MEC: (a) tip displacement; (b) tip velocity.

bound of disturbance estimation error. The model error compensator is designed within the conventional state observer, where a two-step observer design strategy is employed. The major advantage of the model error compensator is that no differentiation of the measured signals is required. The undesired disturbance modal forces are directly cancelled out by the observed disturbance modal forces through the feedback control loop. For ensuring the optimal disturbance attenuation ability of the state feedback control law, the infimal of the H_∞ norm of the defined input/output transfer functions are the design specifications of the static H_∞ state feedback control law. Simulation results show that the H_∞-based controller with the model error compensator can suppress the vibration effectively.

ACKNOWLEDGMENTS

This work was sponsored by National Science Council, ROC, under the grant NCS 89-2212-E-008-038; this support is gratefully acknowledged.

REFERENCES

1. M. J. BALAS 1978 *Journal of Optimization Theory and Applications* **25**, 415–436. Active control of flexible systems.

2. L. MEIROVITCH and H. BARUH 1982 *Journal of Guidance and Control* **5**, 60–66. Control of self-adjoint distributed-parameter systems.
3. L. MEIROVITCH 1990 *Dynamics and Control of Structures*. New York: John Wiley & Sons.
4. D. ERTUR, Y. LI and C. D. RAHN 1979 *Transaction of the American Society of Mechanical Engineers, Journal of Vibration and Acoustics* **121**, 440–445. Adaptive vibration isolation for flexible structures.
5. S. CHOURA 1995 *Transaction of the American Society of Mechanical Engineers, Journal of Dynamic Systems, Measurement, and Control* **117**, 155–164. Control of flexible structures with the confinement of vibrations.
6. M. HOU and P. C. MULLER 1992 *IEEE Transactions on Automatic Control* **37**, 871–875. Design of observers for linear systems with unknown inputs.
7. Y. PARK and J. L. STEIN 1988 *International Journal of Control* **48**, 1122–1136. Closed-loop, state inputs observer for systems with unknown inputs.
8. J. F. TU and J. L. STEIN 1998 *International Journal of Control* **69**, 329–345. Model error compensator for observer design.
9. K. ZHOU and P. P. KHARGONEKAR 1988 *Systems & Control Letters* **11**, 85–91. An algebraic Riccati equation approach to H_∞ optimization.
10. K. ZHOU and J. C. DOYLE 1998 *Essentials of Robust Control*. Englewood Cliffs, NJ: Prentice-Hall International Inc.
11. L. MEIROVITCH 1967 *Analytical Methods in Vibration*. New York: The MacMillan Company.
12. L. MEIROVITCH and H. BARUH 1985 *Journal of Guidance, Control, and Dynamics* **8**, 707–716. The implementation of modal filters for control of structures.
13. P. J. MOYLAN 1977 *IEEE Transactions on Automatic Control* **22**, 74–78. Stable inversion of linear system.
14. G. GU and P. MISRA 1994 *Journal of Guidance, Control, and Dynamics* **17**, 145–152. Disturbance attenuation and H_∞ optimization with linear output feedback control.
15. J. E. DENNIS JR and D. J. WOODS 1987 *SIAM Journal on computing* **16**, 116–122. New computing environments: microcomputers in large-scale computing.